A Method of Moments Solution for Electromagnetic Scattering by Inhomogeneous Dielectric Bodies of Revolution

Andrzej A. Kucharski

***Abstract*—A method of calculating the electromagnetic scattering from and internal field distribution of inhomogeneous dielectric bodies of revolution (BOR) is presented. The method uses typical mode-by-mode solution scheme. The electric flux density is chosen as the unknown quantity, which, together with the special construction of basis and testing functions, enables considerable reduction of the number of unknowns. A key element in this technique is expressing of the azimuthal field components of basis functions in terms of transverse components. A Galerkin testing procedure is used, with special attention put on the efficiency of calculating scalar potential term. Results of calculation for a few classes of dielectric bodies are given and compared with calculations done by other authors.**

***Index Terms*—Dielectric bodies, integral equations, method of moments (MoM).**

I. Introduction

THE problem of scattering of electromagnetic waves by dielectric bodies has been extensively studied by many authors because of its importance in areas such as propagation through rain or snow, medical diagnostics, power absorption in biological bodies, performance of antennas in the presence of dielectric inhomogenity. Especially important is the problem of the rigorous solution of Maxwell equations in the situation when the size of dielectric body is comparable to the wavelength. In this intermediate size region (resonance region) asymptotic methods developed for large or very small bodies cannot be used.

The era of using computer techniques to solve dielectric interaction problems began with the early works of Richmond [1]. Then a great number of methods have been developed for scattering problems [2]–[22]. A special attention is usually paid into those of these methods which use a method of moments (MoM) as the solution scheme [4]–[16]. More recently, a number of hybrid methods [17]–[22] have been proposed, which use the method of moments to properly model radiation condition at the boundary of dielectric region and another technique like finite-element method to model fields inside the region.

In MoM methods, some have been developed for homogeneous [4]–[9], partially homogeneous [10]–[12] or heterogeneous [13]–[16] bodies. In three-dimensional (3-D) models the number of unknowns in matrix equation is usually very large. Therefore, researchers often make use of certain symmetries present in some classes of objects in order to reduce the total number of unknowns. Among those techniques the case of bodies of revolution (BOR) plays an important role [4]–[8], [10]–[12].

Among methods developed for BORs, some concern homogeneous bodies [4]–[8], other inhomogeneous ones [10]–[12], however, most of methods use surface currents in order to satisfy boundary conditions. This leads to serious computational problems, when the great number of very small homogeneous parts has to be treated in the model. This is particularly true, when one wants to model objects with continuously varying dielectric constant. Up until now, mainly hybrid methods mentioned before are well suited for solving such problems, which usually seriously complicates the solution scheme.

Recently, the works of Viola [23], [24] have given a theoretical background for efficient modeling of highly heterogeneous BORs using the MoM techniques. Electric field integral equations (EFIEs) presented have the feature that differential operators do not act on field components, which enables applying simple expansion scheme (pulse-basis functions). However, it is done with the assumption that the dielectric constant ε_r is a well-behaved (continuously differentiable) function of position. In fact, it means that incorporating for example step discontinuities in permittivity profiles requires taking into account additional surface integrals [25].

In this paper, another attitude is presented having similar to Viola's solution efficiency factors (reducing the number of unknowns). The main features of this solution can be summarized as follows:

1) differentiation operators acting on fields are left in equations;
2) piecewise constant permittivity profile is assumed;
3) basis functions with linear capabilities are used in expansion scheme; this allows to avoid convergence problems mentioned in [26];
4) basis functions for nonzeroth modes are divergenceless, which is achieved by applying Gauss' law and calculating azimuthal field components from transverse ones [23];
5) zeroth mode equations for azimuthal and transverse components are decoupled and solved separately;
6) solution procedure remains within convenient mixed potential integral equation (MPIE) scheme;

Manuscript received October 16, 1997; revised May 4, 2000. This work was supported in part by the State Committee for Scientific Research of Poland under Grant 8T11D02311.

The author is with the Radio Department, Institute of Telecommunications and Acoustics, Wrocław University of Technology, 50-370 Wrocław, Poland.

Publisher Item Identifier S 0018-926X(00)07707-3.

7) Galerkin testing is used, which allows to integrate by parts and efficiently calculate matrix components resulting from scalar potential term [15].

In the solution scheme, we generally follow the procedure given in [15] for arbitrary 3-D bodies.

II. Problem Formulation

A. Volume Integral Equation

Let us assume, that a lossy, inhomogeneous, dielectric body with the volume V and complex dielectric constant $\hat{\varepsilon}(\boldsymbol{r}) = \varepsilon(\boldsymbol{r}) - j\sigma(\boldsymbol{r})/\omega$, where ε and σ are the medium permittivity and conductivity at position $\boldsymbol{r}$, is illuminated by an incident field $\boldsymbol{E}^i$, defined as the field in the absence of the body.

In the presence of the body, the total electric field consists of "incident" and "scattered" field

$$\boldsymbol{E}(\boldsymbol{r}) = \boldsymbol{E}^i(\boldsymbol{r}) + \boldsymbol{E}^s(\boldsymbol{r}) \tag{1}$$

the scattered field being excited by the polarization current $\boldsymbol{J}$

$$\boldsymbol{J}(\boldsymbol{r}) = j\omega\left[\hat{\varepsilon}(\boldsymbol{r}) - \varepsilon_0\right]\boldsymbol{E}(\boldsymbol{r}). \tag{2}$$

$\boldsymbol{E}^s$ is related to the polarization current $\boldsymbol{J}$ through the following formulas:

$$\boldsymbol{E}^s(\boldsymbol{r}) = -j\omega\boldsymbol{A}(\boldsymbol{r}) - \nabla\Phi(\boldsymbol{r}) \tag{3}$$

$$\boldsymbol{A}(\boldsymbol{r}) = \frac{\mu_0}{4\pi}\int_V \boldsymbol{J}(\boldsymbol{r}')\,G(\boldsymbol{r},\boldsymbol{r}')\,dv' \tag{4}$$

$$\Phi(\boldsymbol{r}) = \frac{1}{4\pi\varepsilon_0}\int_V q(\boldsymbol{r}')\,G(\boldsymbol{r},\boldsymbol{r}')\,dv' \tag{5}$$

where

$$G(\boldsymbol{r},\boldsymbol{r}') = \frac{e^{-jk_0|\boldsymbol{r}-\boldsymbol{r}'|}}{|\boldsymbol{r}-\boldsymbol{r}'|} \tag{6}$$

$$k_0 = \omega\sqrt{\varepsilon_0\mu_0} = 2\pi/\lambda_0. \tag{7}$$

The charge density $q(\boldsymbol{r})$ is related to the polarization current in (2) by the continuity equation

$$\nabla\cdot\boldsymbol{J}(\boldsymbol{r}) = -j\omega q(\boldsymbol{r}). \tag{8}$$

Equation (1) is, in fact, the integro-differential equation for the polarization current $\boldsymbol{J}$. However, following [15], it is convenient to take as the unknown quantity the electric flux density

$$\boldsymbol{D} = \hat{\varepsilon}\boldsymbol{E} \tag{9}$$

which has a continuous normal component at media interfaces and is divergenceless. This second feature will be extensively used in the construction of basis and testing functions.

We can now express $\boldsymbol{J}$ in terms of $\boldsymbol{D}$

$$\boldsymbol{J}(\boldsymbol{r}) = j\omega\kappa(\boldsymbol{r})\boldsymbol{D}(\boldsymbol{r}) \tag{10}$$

where we define the *contrast ratio* [15]

$$\kappa(\boldsymbol{r}) = \frac{\hat{\varepsilon}(\boldsymbol{r}) - \varepsilon_0}{\hat{\varepsilon}(\boldsymbol{r})} \tag{11}$$

which accounts for discontinuities in the normal component of $\boldsymbol{J}$ at media interfaces.

B. Expansion of VIE Into Modes

Up to this point we have made no use of the fact the body of interest has a rotational symmetry. Taking advantage of this feature, we can expand all currents, fields, and scalar Green's functions in Fourier series in ϕ [8]. Thus, we have

$$\boldsymbol{E}^i = \sum_{m=-\infty}^{\infty}\boldsymbol{E}^i_m(\rho,z)\,e^{jm\phi} \tag{12}$$

$$\boldsymbol{J} = \sum_{m=-\infty}^{\infty}\boldsymbol{J}_m(\rho,z)\,e^{jm\phi} \tag{13}$$

$$\boldsymbol{D} = \sum_{m=-\infty}^{\infty}\boldsymbol{D}_m(\rho,z)\,e^{jm\phi} \tag{14}$$

$$G(\rho,z,\rho',z',\phi-\phi') = \frac{e^{-jk_0R}}{R} = \frac{1}{2\pi}\sum_{m=-\infty}^{\infty}G_m(\rho,z,\rho',z')e^{jm(\phi-\phi')} \tag{15}$$

$$G_m(\rho,z,\rho',z') = \int_0^{2\pi}G(\rho,z,\rho',z',\alpha)e^{-jm\alpha}d\alpha. \tag{16}$$

Expansion (15) follows from the fact that $R = |\boldsymbol{r}-\boldsymbol{r}'|$ is periodic in the variable $(\phi-\phi')$.

Substituting the expansions into formulas (1)–(10) and invoking the ortogonality of azimuthal harmonics, we get

$$\boldsymbol{E}_m(\rho,z) = \boldsymbol{E}^i_m(\rho,z) + \boldsymbol{E}^s_m(\rho,z) \tag{17}$$

$$\boldsymbol{J}_m(\rho,z) = j\omega\left[\hat{\varepsilon}(\rho,z) - \varepsilon_0\right]\boldsymbol{E}_m(\rho,z) \tag{18}$$

$$\boldsymbol{E}^s_m(\rho,z) = -j\omega\boldsymbol{A}_m(\rho,z) - \nabla_m\Phi_m(\rho,z) \tag{19}$$

where

$$\boldsymbol{A}_m = \frac{\mu_0}{4\pi}\int_T\overline{\overline{\Gamma}}_m\boldsymbol{J}_m\rho'\,dt' \tag{20}$$

$$\overline{\overline{\Gamma}}_m = \begin{bmatrix}\Gamma^m_{\rho\rho} & \Gamma^m_{\rho z} & \Gamma^m_{\rho\phi}\\ \Gamma^m_{z\rho} & \Gamma^m_{zz} & \Gamma^m_{z\phi}\\ \Gamma^m_{\phi\rho} & \Gamma^m_{\phi z} & \Gamma^m_{\phi\phi}\end{bmatrix} = \begin{bmatrix}\dfrac{G_{m-1}+G_{m+1}}{2} & 0 & \dfrac{G_{m-1}-G_{m+1}}{2j}\\ 0 & G_m & 0\\ \dfrac{G_{m+1}-G_{m-1}}{2j} & 0 & \dfrac{G_{m-1}+G_{m+1}}{2}\end{bmatrix}. \tag{21}$$

In the above formulas vector components are taken in the (ρ, z, ϕ) order. The integration in (20) is on the transverse surface of the BOR (see Fig. 1).

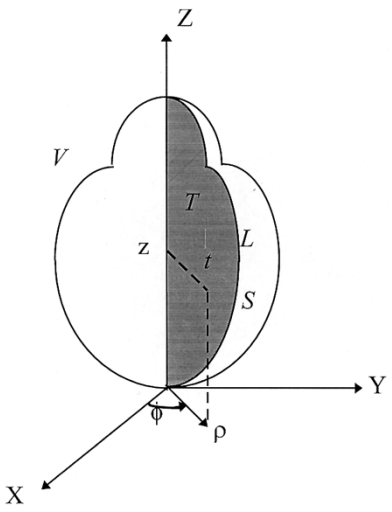

Fig. 1. Body of revolution and coordinate system.

The scalar potential is defined as

$$\Phi_m = \frac{1}{4\pi\varepsilon_0}\int_T q_m G_m \rho'\, dt' \tag{22}$$

where the electric charge density q_m is related to the current $\boldsymbol{J}_m$ through

$$q_m = -\frac{1}{j\omega}\nabla_m \cdot \boldsymbol{J}_m = -\frac{1}{j\omega}\left[\frac{1}{\rho'}\frac{\partial(\rho' J_m^{\rho})}{\partial\rho} + \frac{\partial J_m^z}{\partial z} + \frac{jm}{\rho'} J_m^{\phi}\right]. \tag{23}$$

In (23) we introduce the harmonic divergence. Additionally, we define the harmonic gradient operator

$$\nabla_m \Phi_m = \hat{\rho}\,\frac{1}{\rho}\frac{\partial(\rho\Phi_m)}{\partial\rho} + \hat{z}\,\frac{\partial\Phi_m}{\partial z} + \hat{\phi}\,\frac{jm}{\rho}\,\Phi_m. \tag{24}$$

C. Basis Functions Development

As mentioned before, the electric flux density has been chosen as the unknown quantity in the moment method solution. Thus, we have

$$\boldsymbol{D}(\boldsymbol{r}) = \sum_{i=1}^{N} D_i \boldsymbol{f}_i(\boldsymbol{r}) \tag{25}$$

or, for the mth mode

$$\boldsymbol{D}_m(\rho, z) = \sum_{i=1}^{N} D_{mi}\boldsymbol{f}_{mi}(\rho, z) \tag{26}$$

where N is the total number of basis functions.

The main purpose in the process of basis functions development is to impose on the basis set the condition that $\boldsymbol{D}$ is divergenceless. Satisfying this condition allows to reduce the total number of unknowns.

Thus, we have

$$\nabla_m \cdot \boldsymbol{f}_m = \frac{1}{\rho}\frac{\partial(\rho f_m^{\rho})}{\partial\rho} + \frac{\partial f_m^z}{\partial z} + \frac{jm}{\rho} f_m^{\phi} = 0. \tag{27}$$

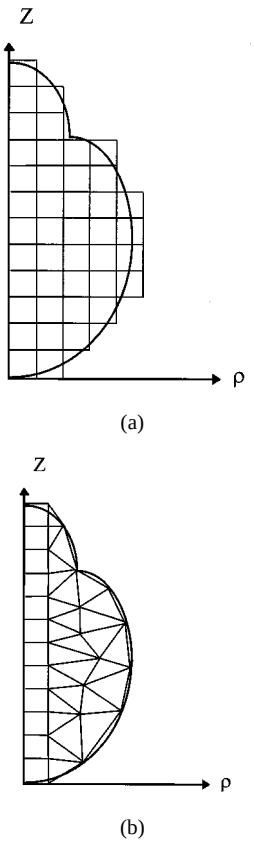

Fig. 2. Discretization of the transverse plane of the body. (a) Rectangular basis functions. (b) Rectangular and triangular basis functions.

It is easy to find, that for all modes except $m = 0$ we can derive the ϕ component of $\boldsymbol{f}_m$ taking

$$f_m^{\phi} = -\frac{\rho}{jm}\left[\frac{1}{\rho}\frac{\partial(\rho f_m^{\rho})}{\partial\rho} + \frac{\partial f_m^z}{\partial z}\right]. \tag{28}$$

It means that in the process of solution of (17) we can deal only with "transverse" components. It is the desired feature of number of unknowns reduction. The zeroth mode has to be treated separately and the solution for this case will be discussed later on.

We can note that in the divergence relation (27) the ρ-directed field component is multiplied by ρ, while the z-directed component appears alone, i.e., without the ρ multiplier. Thus, as will be seen in the subsequent paragraph, it is useful to use different expansions for both components of $\boldsymbol{D}$. When the "rooftop" function [8] are used to represent the transverse fields, it is then appropriate to expand ρD_ρ using "radial" rooftop functions, while it is appropriate to expand D_z directly in z-directed rooftop functions. The consequence of this is the fact that a constant variation in ρ is assured for both field components in the immediate neighborhood of the z-axis.

D. Basis Functions on Rectangular Domains

Assuming that the transverse surface of the BOR is divided into small rectangles [see Fig. 2(a)] with piecewise constant dielectric parameters, we define two sets of basis functions (see Fig. 3 for notations) as follows:

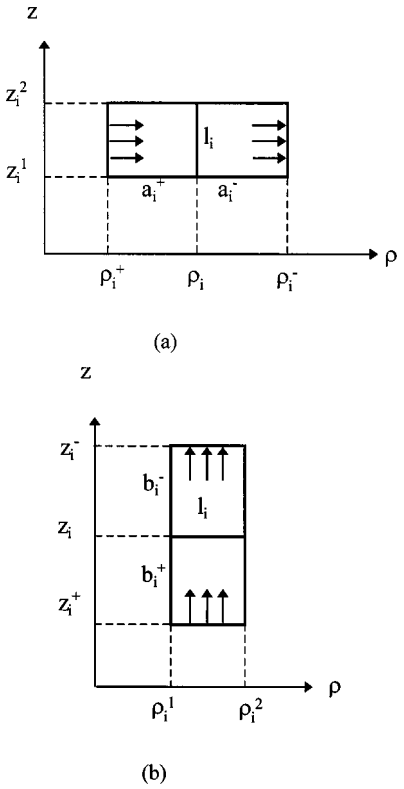

Fig. 3. Rectangle pairs and geometrical parameters associated with rectangular basis functions. (a) Type ρ. (b) Type z.

1) type ρ functions defined as

$$\boldsymbol{g}_{mi}(\rho, z) = \begin{cases} \hat{\rho}\dfrac{1}{\rho}\dfrac{(\rho-\rho_i^+)}{a_i^+} - \hat{\phi}\dfrac{1}{jma_i^+}, & \rho \in (\rho_i^+, \rho_i),\ z \in (z_i^1, z_i^2) \\ \hat{\rho}\dfrac{1}{\rho}\dfrac{(\rho_i^- - \rho)}{a_i^-} + \hat{\phi}\dfrac{1}{jma_i^-}, & \rho \in (\rho_i, \rho_i^-),\ z \in (z_i^1, z_i^2) \\ 0, & \text{otherwise} \end{cases} \tag{29}$$

2) type z functions defined as

$$\boldsymbol{h}_{mi}(\rho, z) = \begin{cases} \hat{z}\dfrac{(z-z_i^+)}{b_i^+} - \hat{\phi}\dfrac{\rho}{jmb_i^+}, & \rho \in (\rho_i^1, \rho_i^2),\ z \in (z_i^+, z_i) \\ \hat{z}\dfrac{(z_i^- - z)}{b_i^-} + \hat{\phi}\dfrac{\rho}{jmb_i^-}, & \rho \in (\rho_i^1, \rho_i^2),\ z \in (z_i, z_i^-) \\ 0, & \text{otherwise} \end{cases} \tag{30}$$

If the internal edge of the basis function is on the body contour, the basis function is defined only on rectangle interior to T. No basis functions are associated with the edges lying on the z axis.

It can be easily checked using (27) that functions (29) and (30) are divergenceless. It should be remembered that "modal" basis functions should be understood in global expansion scheme as multiplied by $\exp(jm\phi)$ factor.

Thus, (26) now takes the form

$$\boldsymbol{D}_m(\rho, z) = \sum_{i=1}^{N_\rho} D_{mi}^{\rho}\boldsymbol{g}_{mi}(\rho, z) + \sum_{i=1}^{N_z} D_{mi}^{z}\boldsymbol{h}_{mi}(\rho, z) \tag{31}$$

where N_ρ and N_z are the numbers of functions defined by (29) and (30), respectively. Of course, $N_\rho + N_z = N$.

The corresponding currents associated with basis functions can be calculated from (10). The total modal current at given point can be expressed as

$$\begin{aligned} \boldsymbol{J}_m(\rho, z) = {} & j\omega \sum_{i=1}^{N_\rho} D_{mi}^{\rho}\kappa(\rho, z)\,\boldsymbol{g}_{mi}(\rho, z) \\ & + j\omega \sum_{i=1}^{N_z} D_{mi}^{z}\kappa(\rho, z)\,\boldsymbol{h}_{mi}(\rho, z). \end{aligned} \tag{32}$$

By substituting (8) with (32) the charge density is found to be represented by

$$\begin{aligned} q_m(\rho, z) = {} & -\sum_{i=1}^{N_\rho} D_{mi}^{\rho}\kappa(\rho, z)\,\nabla_m \cdot \boldsymbol{g}_{mi}(\rho, z) \\ & - \sum_{i=1}^{N_\rho} D_{mi}^{\rho}\boldsymbol{g}_{mi}(\rho, z) \cdot \nabla_m \kappa(\rho, z) \\ & - \sum_{i=1}^{N_z} D_{mi}^{z}\kappa(\rho, z)\,\nabla_m \cdot \boldsymbol{h}_{mi}(\rho, z) \\ & - \sum_{i=1}^{N_z} D_{mi}^{z}\boldsymbol{h}_{mi}(\rho, z) \cdot \nabla_m \kappa(\rho, z). \end{aligned} \tag{33}$$

The first and third summations in (33) represent volume charge densities, which, in the case of divergenceless functions, (29) and (30) are simply equal to zero. The second and fourth summations, assuming piecewise constant profile of the contrast ratio κ, represent surface charge densities associated with basis functions

$$q_{smi}^{\rho}(\rho, z) = \begin{cases} \dfrac{1}{\rho} D_{mi}^{\rho}\left(\kappa_i^{\rho+} - \kappa_i^{\rho-}\right), & (\rho, z) \in l_i \\ 0, & \text{otherwise} \end{cases} \tag{34}$$

$$q_{smi}^{z}(\rho, z) = \begin{cases} D_{mi}^{z}\left(\kappa_i^{z+} - \kappa_i^{z-}\right), & (\rho, z) \in l_i \\ 0, & \text{otherwise} \end{cases} \tag{35}$$

where l_i in (34) and (35) is associated with ρ-type and z-type basis functions, respectively.

From above equations it is easy to find that calculations of the scalar potential do not require calculating the surface integrals, because the integral in (22) now becomes a contour integral.

E. Basis Functions on Triangular Domains

For triangular domains, basis functions similar to Rao–Wilton–Glisson (RWG) functions [27] can be easily applied. Again we define basis functions associated with the edges rather than with triangles, which span over two triangles (like classical rooftop functions over two rectangles).

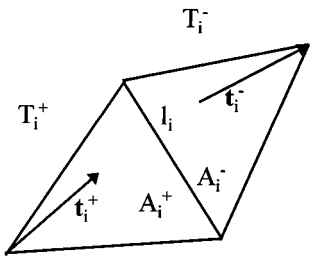

Fig. 4. Triangle pair and geometrical parameters associated with triangular basis function.

Expanding $\rho \boldsymbol{D}_m^t(\rho, z)$ into RWG functions and calculating D_m^ϕ from (28), we get the basis function definition

$$\boldsymbol{f}_{mi}(\rho, z) = \begin{cases} \boldsymbol{t}_i^+ \dfrac{1}{\rho} \dfrac{l_i}{2A_i^+} - \hat{\phi} \dfrac{1}{jm} \dfrac{l_i}{A_i^+}, & (\rho, z) \in T_i^+ \\ \boldsymbol{t}_i^- \dfrac{1}{\rho} \dfrac{l_i}{2A_i^-} + \hat{\phi} \dfrac{1}{jm} \dfrac{l_i}{A_i^-}, & (\rho, z) \in T_i^- \\ 0, & \text{otherwise} \end{cases} \tag{36}$$

where the $\boldsymbol{t}_i^\pm$ vectors responsible for the transverse fields are defined in Fig. 4.

Formulas similar to (32)–(35) for representing currents and charges can be easily obtained.

It should be noted that functions (36) are not able to represent correctly fields in subdomains in the immediate vicinity of z-axis. It is first because of piecewise constant character of the RWG function in the direction perpendicular to current flow which results, after multiplying by $1/\rho$, with incorrect representation of D_z component near the z-axis. Second, because of similar reasons, no basis function can be defined on triangle edges lying on the z-axis. Taking into account that in order to represent field in any direction all three basis functions associated with each triangle must be used, we find that fields in the vicinity of z-axis cannot be correctly represented by functions defined in (36). On the other hand, omitting $1/\rho$ term in the definition results in much complication of divergence formulas which obviously cancels one of main advantages of using RWG functions.

One solution is to combine functions defined on rectangles for representation of fields near the z-axis with functions defined on triangles for the rest of the body. This would, however, require defining additional "mixed" basis functions for edges separating rectangles and triangles [see Fig. 2(b)].

In the examples in the next section only simple "rooftop" basis functions defined on rectangles have been applied, because authors main interest was to show the idea of basis function development rather than to look for the most optimal representations of bodies curvatures.

F. Testing Procedure

In order to get unknown coefficients of the electric flux density expansion equation (17) must be tested to reduce it to the set of simultaneous linear equations. In this work, the Galerkin procedure has been applied, together with the scalar product defined as

$$\langle \boldsymbol{f}, \boldsymbol{g} \rangle = \int_V \boldsymbol{f} \cdot \boldsymbol{g}^* \, dv. \tag{37}$$

For the mode m we get

$$\langle \boldsymbol{f}_m, \boldsymbol{g}_m \rangle = \int_T \int_0^{2\pi} \boldsymbol{f}_m(\rho, z) e^{jm\phi} \cdot \boldsymbol{g}_m^*(\rho, z) e^{-jm\phi} \rho \, d\phi \, dt \tag{38}$$

which after performing the ϕ integration results in

$$\langle \boldsymbol{f}_m, \boldsymbol{g}_m \rangle = 2\pi \int_T \boldsymbol{f}_m(\rho, z) \cdot \boldsymbol{g}_m^*(\rho, z) \rho \, dt \tag{39}$$

where T is the "transverse" area of the body shown in Fig. 1.

Equation (17) tested with the function $\boldsymbol{f}_{mj}$, either ρ or z type, takes the form

$$\left\langle \frac{\boldsymbol{D}_m}{\hat{\varepsilon}}, \boldsymbol{f}_{mj} \right\rangle + j\omega \langle A_m, \boldsymbol{f}_{mj} \rangle + \langle \nabla_m \Phi_m, \boldsymbol{f}_{mj} \rangle = \langle E_m^i, \boldsymbol{f}_{mj} \rangle \tag{40}$$

which, taking into account expansion (31), represents the desired matrix equation with the vector of unknown coefficients $\{D_{mi}^p\}$, $p = \rho, z$. The integrations that must be performed to calculate elements of the moment matrix are on the T surface, except for the scalar potential term. The surface integrations are performed numerically, assuming that each triangle function in (29) and (30) is approximated with pulse functions [29]. This results in four points per rectangle integration scheme.

It is well known [28], [29] that the modal Green's function G_m has an integrable singularity. Thus, while calculating "self terms" in (40), the integrations in the immediate vicinity of singular points must be performed analytically.

Some attention should be given to the scalar potential term in (40). The direct form of this term has an undesirable feature of acting with gradient operation on Φ_m. This, however, can be eliminated by the use of formula [15]

$$\langle \nabla \Phi, \boldsymbol{f} \rangle = \int_S \Phi \boldsymbol{f}^* \cdot \hat{n} \, dS - \int_V \Phi \nabla \cdot \boldsymbol{f}^* \, dv \tag{41}$$

which, considering that the weighting functions are divergenceless, after putting into "modal" form gives

$$\langle \nabla_m \Phi_m, \boldsymbol{f}_m \rangle = 2\pi \int_L \Phi(\rho, z) \boldsymbol{f}_m^*(\rho, z) \cdot \hat{n} \rho \, dl \tag{42}$$

where L is the contour of T.

In (41) and (42), $\hat{n}$ is the unit vector normal to the surface S or contour L, respectively.

Thus, only testing functions associated with the contour of the body give the nonzero contribution into moment matrix elements. This fact has reduced considerably amount of computations associated with the scalar potential term.

Again, care must be taken while calculating "self-term" elements of the matrix because of Green's function singularity, which requires some analytical integration. It is worth pointing out that the singularity problem in this case can be avoided by surrounding the body with the layer of "empty" basis functions

(which means subdomains with dielectric permitivity equal to that of surrounding space). In this case, there is no surface charge density on the S surface, which results in the fact that all "self-term" elements are explicitly equal to zero. Both cases has been tried in practice giving coinciding results.

G. Zeroth Mode

The technique of basis function construction presented above cannot be used in the case of $m = 0$. In this case, however, it can be noted that

1) there is no charge associated with the azimuthal field component;
2) modal gradient operator has no azimuthal component;
3) $G_{-1} = G_1$, so the $\rho\phi$ and $\phi\rho$ components of $\overline{\overline{\Gamma}}$ matrix (21) are zero.

Thus, for zeroth mode, (17) decouples into two independent equations concerning transverse and azimuthal field components. These equations can then be solved separately.

Solving the equation for transverse field components, the author has used the same transverse field representation as in the previous subsection. However, one must remember, that basis functions constructed in this manner are no longer divergenceless. It means that we must take into account volume charges, which appear in (33) while computing the scalar potential. Next, also the second integral in (41) has to be considered when calculating the scalar potential contribution to impedance matrix elements. The mentioned steps cause in fact enforcing the zero divergence condition numerically.

The equation for the azimuthal mode has very simple form, because it does not have the scalar potential term. In present work, it has been solved numerically using pulse basis functions and the Galerkin testing scheme.

Note that because of the equations decoupling, we never have to solve system of linear equation with more unknowns than in the case of nonzero modes. It means that the main advantage of the method is, in this case, preserved.

III. Numerical Results

In order to check the method described in the previous section, it has been applied to some problems for which solutions, either analytical or numerical, obtained by other authors are available. Most of those solutions concern homogeneous or partially homogeneous bodies. In all calculations basis functions defined on rectangular domains have been used.

As a first example, homogeneous dielectric sphere has been considered. Next, a layered sphere has been modeled and, finally, the radar cross sections of bodies with simple shapes have been calculated and compared to results of methods developed by other authors.

In all examples, the incident field has been assumed to be a plane wave. This requires applying formulas for plane wave expansion into modes. Similarly, when calculating radar cross sections, the far field from individual modes has to be computed. Formulas for these expansions can be easily obtained from those presented for example in [28] or [29] and will be not repeated here.

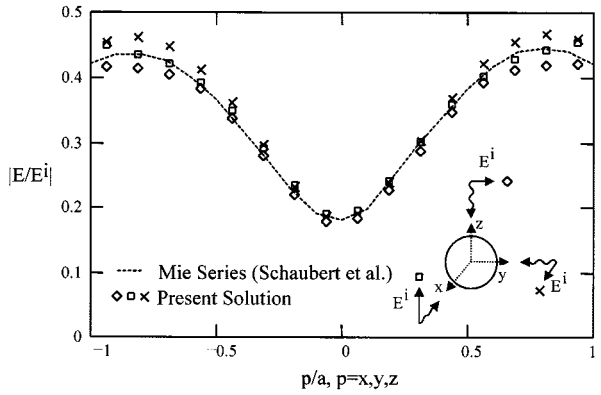

Fig. 5. Field along axis of incidence inside dielectric sphere; $\varepsilon_r = 36$, $k_0 a = 0.408$.

A. Dielectric Sphere

A simple sphere model, with discretization similar to that of Fig. 2(a), has been used to calculate the electric field inside a dielectric sphere. In the model eight squares per the sphere radius have been used, which corresponds to 216 unknowns. First, axial incidence of the incident field has been assumed, which requires performing computations only for the -1 and $+1$ modes. Field calculations for low frequencies have shown that the electric field is within 5% of $3/(\varepsilon_r + 2)$ times the incident field, which is the theoretical value.

At higher frequencies, the typical standing wave behavior has been observed. In Fig. 5 the comparison of results with analytical solution [15] is presented for the sphere with $k_0 a = 0.408$. One can see that the agreement is good. In order to verify procedures for the zeroth mode and more sophisticated modal expansions, the same calculations for different angles of incidence and polarizations has been performed. The small picture in the corner of Fig. 5 relates symbols used in the plot to the different scattering situations. The simplest case with the incidence along z-axis is denoted with the diamond symbols. Again, very good agreement has been obtained which validates all procedures described in the previous section. The reader can notice that calculated solutions slightly differ from each other and from analytical solution near the ends of the plot. It is caused by rather crude approximation of the sphere surface within applied model.

Field distributions for the layered sphere are presented in Fig. 6. The calculations have been done for two grids. The solutions 1 and 2 denote 8 and 16 squares per outer radius of the sphere, respectively. The solution 1 gives some error in the vicinity of the boundary of materials. It is because of nonprecise model of the inner sphere. Solution 2 gives a very good field prediction. It proves improvement of accuracy when the investigated body is modeled using smaller volume elements. Note, that the jump in E_x component calculated along x-axis is perfectly predicted. It is because correct behavior at media interfaces is built-in into the basis functions in the way similar to [15]. It is also worth mentioning that even in the case of the solution 1 the resolution of the model is about twice that of the tetrahedron (full 3-D) model [15]. However, thanks to the rotational symmetry the number of unknowns is only 216 in comparison to 1088 in the tetrahedron model. In solution 2, with the

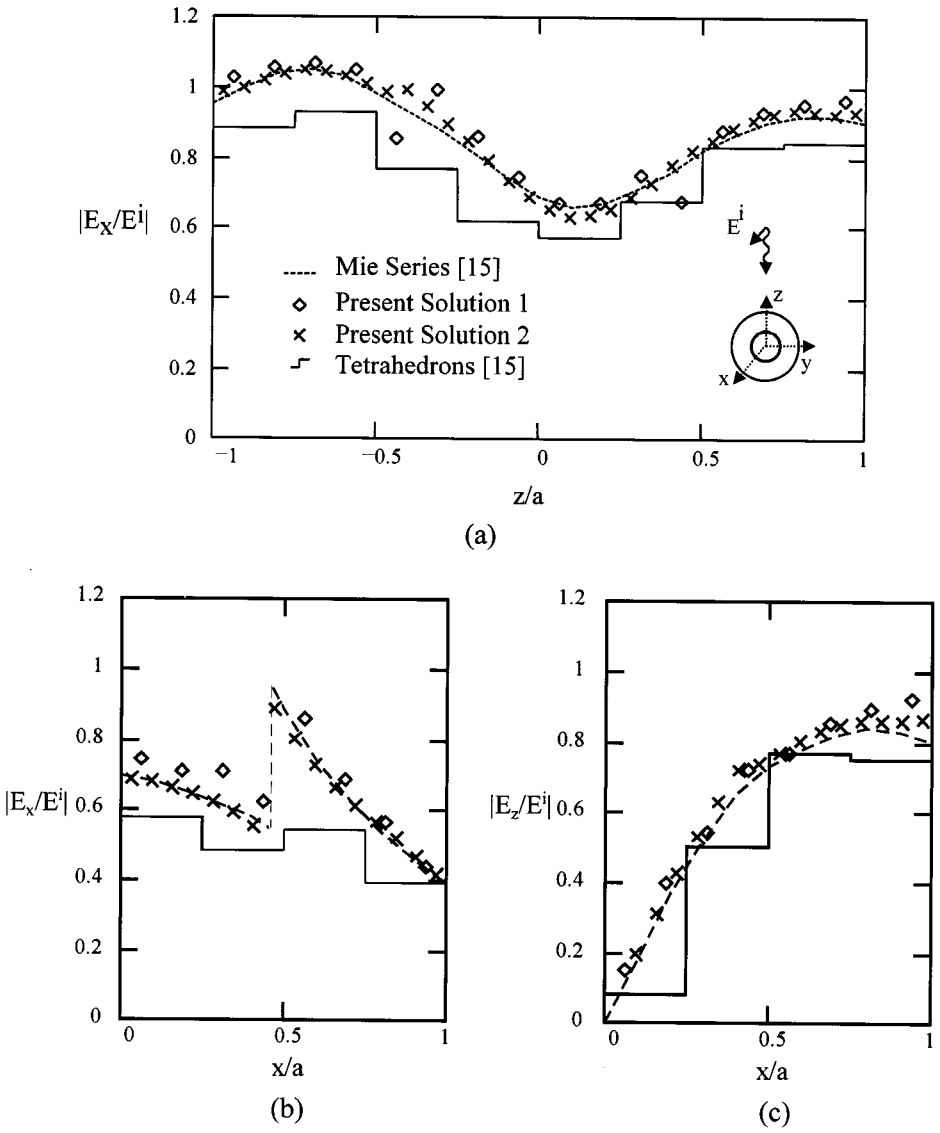

Fig. 6. Fields inside inhomogeneous sphere: $\varepsilon_{r1} = 36$, $k_0 a_1 = 0.3738$, $\varepsilon_{r2} = 9$, $k_0 a_2 = 0.8168$. (a) Relative magnitude of E_x along z axis. (b) Relative magnitude of E_x along x axis. (c) Relative magnitude of E_z along x axis.

resolution doubled in comparison to the solution 1, we have 828 unknowns, which is still less than in the 3-D case.

B. Scattering Calculations

Both because of difficulties to measure field inside dielectric bodies and because of practical importance, the main parameter calculated and published in the literature is the radar cross section. In this work, the radar cross section of a thin dielectric rod has been computed and compared to the results of Richmond [30], Wang and Papanicolopulos [31] and Shaubert *et al.* [15]. The BOR model consists of a single column of rectangular cells (in the transverse plane). The results are presented in Fig. 7, where the agreement again is found to be excellent.

Next, the bistatic radar cross section of a dielectric cylinder has been calculated and compared to data given by Mautz and Harrington [7]. The comparison is done in Fig. 8.

Finally, some calculations of resonant frequencies of dielectric spheres and cylinders have been performed and compared to analytical and numerical results given by Barber *et al.* [32]. In all cases, resonant frequencies predicted with the present method were within 0.5% from those of Barber *et al.*

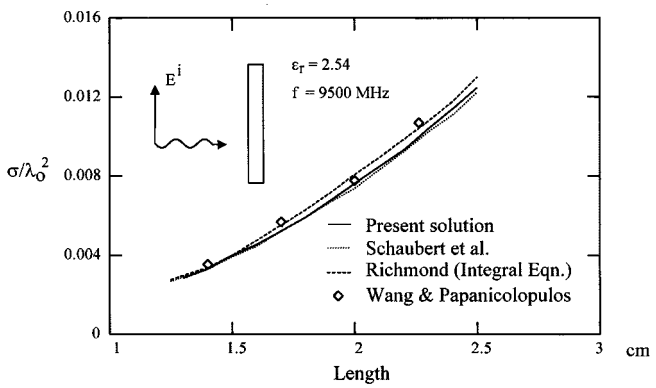

Fig. 7. Radar cross section of a thin dielectric rod: $a = 0.16\,\text{cm} = 0.05\lambda_0$, $\varepsilon_r = 2.54$.

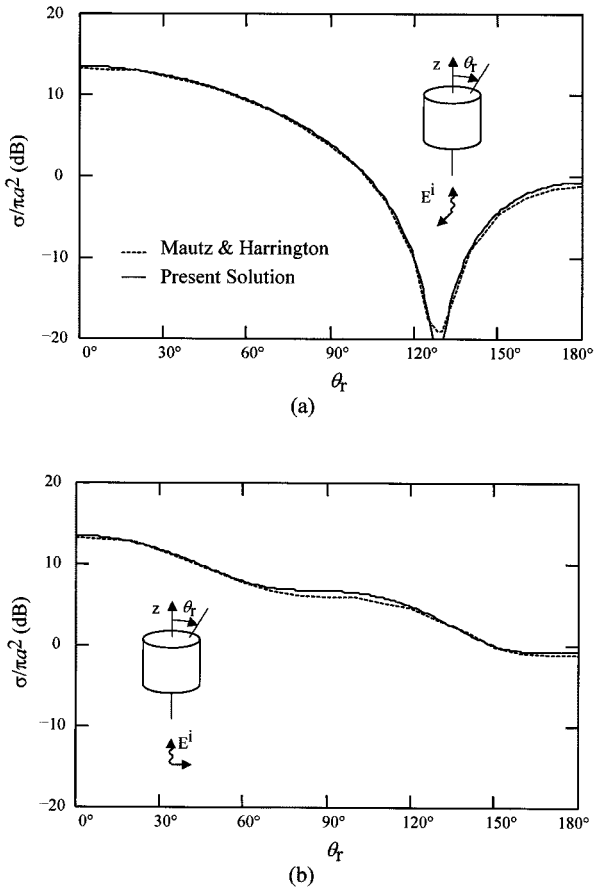

Fig. 8. Plane wave scattering patterns for dielectric cylinder of radius a and height $2a$. $a = 0.25\lambda_0$, $\varepsilon_r = 4$. (a) $\phi\phi$ polarization. (b) $\theta\theta$ polarization.

IV. Summary

An efficient method of calculating the electromagnetic fields scattered from and penetrating into inhomogeneous dielectric bodies of revolution has been presented. The method uses special, divergenceless basis functions defined on rectangular or triangular domains in which the azimuthal component is calculated from transverse ones by the use of Gauss' law. This allows one to considerably reduce the total number of unknowns used in the solution procedure. Following [15] the basis functions automatically incorporate the boundary conditions of the normal component of electric flux density.

The testing procedure used for the method of moments solution is a Galerkin scheme with the typical for bodies-of-revolution procedure of decoupling of the solving process into modes.

Numerical results show that the method gives excellent results both while predicting internal fields distributions and scattered fields.

Finally, it is important that the solution remains within the convenient mixed potential EFIE scheme. Therefore, it is expected that the generalization to the case of multilayered media should not present much theoretical difficulties [33], [34].

References

[1] J. H. Richmond, "Scattering by a dielectric cylinder of arbitrary cross section shape," *IEEE Trans. Antennas Propagat.*, vol. AP-13, pp. 334–341, May 1965.

[2] A. Taflove and M. E. Brodwin, "Computation of the electromagnetic fields and induced temperatures within a model of the microwave-irradiated human eye," *IEEE Trans. Microwave Theory Tech.*, vol. MTT-23, pp. 888–896, Nov. 1975.

[3] R. Holland, L. Simpson, and K. S. Kunz, "Finite-difference analysis of EMP coupling to lossy dielectric structures," *IEEE Trans. Electromagn. Compat.*, vol. EMC-22, pp. 203–209, Aug. 1980.

[4] T. K. Wu and L. L. Tsai, "Scattering from arbitrarily-shaped lossy dielectric bodies of revolution," *Radio Sci.*, vol. 12, pp. 709–718, Sept. 1977.

[5] T. Wu, "Electromagnetic fields and power deposition in body-of-revolution models of man," *IEEE Trans. Microwave Theory Tech.*, vol. MTT-27, pp. 279–283, Mar. 1979.

[6] J. R. Mautz and R. F. Harrington, "H-field, E-field and combined-field solutions for conducting bodies of revolution," *Arch. Elec. Ubertragung.*, vol. 32, pp. 159–164, Apr. 1978.

[7] ——, "Electromagnetic scattering from a homogeneous material body of revolution," *Arch. Elec. Ubertragung.*, vol. 33, pp. 71–80, Feb. 1979.

[8] A. W. Glisson and D. R. Wilton, "Simple and efficient numerical methods for problems of electromagnetic radiation and scattering from surfaces," *IEEE Trans. Antennas Propagat.*, vol. AP-28, pp. 593–603, Sept. 1980.

[9] K. Umashankar, A. Taflove, and S. M. Rao, "Electromagnetic scattering by arbitrary shaped three-dimensional homogeneous lossy dielectric objects," *IEEE Trans. Antennas Propagat.*, vol. AP-34, pp. 758–766, June 1986.

[10] L. N. Medgyesi-Mitschang and C. Eftimiu, "Scattering from axisymmetric obstacles embedded in axisymmetric dielectrics: The method of moments solution," *Appl. Phys.*, vol. 19, pp. 275–285, Feb. 1979.

[11] L. N. Medgyesi-Mitschang and J. M. Putnam, "Electromagnetic scattering from axially inhomogeneous bodies of revolution," *IEEE Trans. Antennas Propagat.*, vol. AP-32, pp. 797–806, Aug. 1984.

[12] S. Govind, D. R. Wilton, and A. W. Glisson, "Scattering from inhomogeneous penetrable bodies of revolution," *IEEE Trans. Antennas Propagat.*, vol. AP-32, pp. 1163–1173, Nov. 1984.

[13] D. E. Livesay and K.-M. Chen, "Electromagnetic fields induced inside arbitrarily shaped biological bodies," *IEEE Trans. Microwave Theory Tech.*, vol. MTT-22, pp. 1273–1280, Dec. 1974.

[14] M. J. Hagmann, O. P. Ghandhi, and C. H. Durney, "Numerical calculation of electromagnetic energy deposition for a realistic model of man," *IEEE Trans. Microwave Theory Tech.*, vol. MTT-27, pp. 804–809, Sept. 1979.

[15] D. H. Schaubert, D. R. Wilton, and A. W. Glisson, "A tetrahedral modeling method for electromagnetic scattering by arbitrarily shaped inhomogeneous dielectric bodies," *IEEE Trans. Antennas Propagat.*, vol. AP-32, pp. 77–85, Jan. 1984.

[16] C. Tsai, H. Massoudi, C. H. Durney, and M. F. Iskander, "A procedure for calculating fields inside arbitrarily shaped inhomogeneous dielectric bodies using linear basis functions with the moment method," *IEEE Trans. Microwave Theory Tech.*, vol. MTT-34, pp. 1131–1139, Nov. 1986.

[17] M. A. Morgan, S. K. Chang, and K. K. Mei, "Coupled azimuthal potentials for electromagnetic field problems in inhomogeneous axially-symmetric media," *IEEE Trans. Antennas Propagat.*, vol. AP-25, pp. 413–417, May 1977.

[18] M. A. Morgan and K. K. Mei, "Finite element computation of scattering by inhomogeneous penetrable bodies of revolution," *IEEE Trans. Antennas Propagat.*, vol. AP-27, pp. 202–214, Mar. 1979.

[19] D. J. Hoppe, L. W. Epp, and J.-F. Lee, "A hybrid symmetric FEM/MOM formulation applied to scattering by inhomogeneous bodies of revolution," *IEEE Trans. Antennas Propagat.*, vol. 42, pp. 798–805, June 1994.

[20] X. Yuan, D. R. Lynch, and J. W. Strohbehn, "Coupling of finite element and moment methods for electromagnetic scattering from inhomogeneous objects," *IEEE Trans. Antennas Propagat.*, vol. 38, pp. 386–393, Mar. 1990.

[21] W. E. Boyse and A. A. Seidl, "A hybrid finite element method for near bodies of revolution," *IEEE Trans. Magn.*, vol. 27, pp. 3833–3836, Sept. 1991.

[22] T. Cwik, C. Zuffada, and V. Jamnejad, "Modeling three-dimensional scatterers using a coupled finite element–integral equation formulation," *IEEE Trans. Antennas Propagat.*, vol. 44, pp. 453–459, Apr. 1996.

[23] M. S. Viola, "A new electric field integral equation for heterogeneous dielectric bodies of revolution," *IEEE Trans. Microwave Theory Tech.*, vol. 43, pp. 230–232, Jan. 1995.

[24] M. S. Viola, "A new electric field integral equation for heterogeneous dielectric bodies of revolution embedded within a stratified medium," *IEEE Trans. Antennas Propagat.*, vol. 43, pp. 1116–1122, Oct. 1995.

[25] J. Volakis, "Alternative field representations and integral equations for modeling inhomogeneous dielectrics," *IEEE Trans. Microwave Theory Tech.*, vol. 40, pp. 604–608, Mar. 1992.
[26] R. F. Harrington, *Field Computation by Moment Methods*. New York: Macmillan, 1968.
[27] S. M. Rao, D. R. Wilton, and A. W. Glisson, "Electromagnetic scattering by surfaces of arbitrary shape," *IEEE Trans. Antennas Propagat.*, vol. AP-30, pp. 409–418, May 1982.
[28] M. G. Andreasen, "Scattering from bodies of revolution," *IEEE Trans. Antennas Propagat.*, vol. AP-13, pp. 303–310, Mar. 1965.
[29] J. R. Mautz and R. F. Harrington, "Radiation and scattering from bodies of revolution," *Appl. Sci. Res.*, vol. 20, pp. 405–435, June 1969.
[30] J. H. Richmond, "Digital computer solutions of the rigorous equations for scattering problems," *Proc. IEEE*, vol. 53, pp. 796–804, Aug. 1965.
[31] J. J. H. Wang and C. Papanicolopulos, "A study of the analysis and measurements of three-dimensional arbitrarily-shaped dielectric scatterers," Rome Air Development Ctr., Rep. RADC-TR-30-372, Dec. 1980.
[32] P. W. Barber, J. F. Owen, and R. K. Chang, "Resonant scattering for characterization of axisymmetric dielectric objects," *IEEE Trans. Antennas Propagat.*, vol. AP-30, pp. 168–172, Mar. 1982.
[33] K. A. Michalski and D. Zheng, "Electromagnetic scattering and radiation by surfaces of arbitrary shape in layered media—Parts I and II," *IEEE Trans. Antennas Propagat.*, vol. AP-38, pp. 335–352, Mar. 1990.
[34] A. K. Abdelmageed and K. A. Michalski, "Analysis of EM scattering by conducting bodies of revolution in layered media using the discrete complex image method," in *Proc. IEEE Antennas Propagat. Soc. Int. Symp.*, vol. 1, Newport Beach, CA, June 1995, pp. 402–405.

Andrzej A. Kucharski was born in Wrocław, Poland, in 1964. He received the M.Sc. and Ph.D. degrees from Wrocław University of Technology, Wrocław, Poland, in 1988 and 1994, respectively.

Since 1993, he has been with the Radio Department, Institute of Telecommunications and Acoustics, Wrocław University of Technology, where he is currently an Assistant Professor. In 1993 and 1994, he spent three months in the European Telecommunications Standards Institute, Sophia Antipolis, France, serving as an expert in the field of the satellite telecommunications. His research interests are primarily in computational electromagnetics, antennas and propagation, and electromagnetic compatibility.